



## Improved Retention Characteristics of Pd-Nanocrystal-Based Nonvolatile Memories by a Simple Timing Technique

Tsung-Kuei Kang,<sup>a,\*</sup> Yun-Feng Chen,<sup>a</sup> Cheng-Li Lin,<sup>a</sup> Fang-Hsing Wang,<sup>b</sup> Han-Wen Liu,<sup>b</sup> Feng-Tso Chien,<sup>a</sup> and Jen-Bin Shi<sup>a</sup>

<sup>a</sup>Department of Electronic Engineering, Feng-Chia University, Taichung, Taiwan

<sup>b</sup>Department of Electrical Engineering and Graduate Institute of Optoelectronic Engineering, National Chung Hsing University, Taichung, Taiwan

By controlling the different initial time of Hf and Al precursor supply, the proposed  $\text{Hf}_x\text{Al}_y\text{O}_z$  tunneling layer with different Al/Hf ratios from 0.21 (top) to 0.06 (bottom) can be fabricated. Regarding Al/SiO<sub>2</sub>/Pd nanocrystals/proposed  $\text{Hf}_x\text{Al}_y\text{O}_z/\text{Si}$ , the proposed  $\text{Hf}_x\text{Al}_y\text{O}_z$  film can prevent stress from Pd nanocrystals and achieve a higher electron current during programming. Regarding the retention characteristics, the final memory windows of 2.5/2.05 V at 25/90°C can be obtained, respectively. Programmed and erased with  $\pm 10$  V/100 ms, the device shows a memory window of 2.4 V after 10<sup>4</sup> cycles for a 25°C test.

© The Author(s) 2015. Published by ECS. This is an open access article distributed under the terms of the Creative Commons Attribution 4.0 License (CC BY, <http://creativecommons.org/licenses/by/4.0/>), which permits unrestricted reuse of the work in any medium, provided the original work is properly cited. [DOI: 10.1149/2.0071512ssll] All rights reserved.

Manuscript submitted May 14, 2015; revised manuscript received September 23, 2015. Published September 30, 2015.

Regarding high-k dielectrics, HfO<sub>2</sub> shows a higher dielectric constant as compared to SiO<sub>2</sub>.<sup>1-3</sup> However, the crystallization temperature of HfO<sub>2</sub> is very low and easily results in a higher leakage current. Previous research indicated the crystallization temperature of HfO<sub>2</sub> can be significantly increased by adding Al to the film.<sup>4</sup> Moreover, adding Al to HfO<sub>2</sub> is found to increase the Si/dielectric interfacial stability.<sup>5</sup> Regarding memory application,  $\text{Hf}_x\text{Al}_y\text{O}_z$  film was served in the storage layer of the nonvolatile memory (NVM) device and good memory characteristics were achieved.<sup>6</sup> Previous studies showed the embedded metal nanocrystals (NCs) in the dielectric of a NVM device improved the data retention characteristics.<sup>7-11</sup> However, previous study reported that a huge stress induced by metal NCs in the SiO<sub>2</sub> tunneling layer led to a worse retention characteristic and a small memory window because of many shallow traps in the SiO<sub>2</sub> tunneling layer. Therefore, to reduce the shallow traps induced by metal NCs was an important issue.<sup>12</sup> A high density of Pd NCs was easily formed on the  $\text{Hf}_x\text{Al}_y\text{O}_z$  tunneling layer, so the NVM with Pd NCs storage layer was also studied.<sup>12-13</sup> Instead of SiO<sub>2</sub>, the  $\text{Hf}_x\text{Al}_y\text{O}_z$  was served as the tunneling layer, the retention characteristic in Pd NCs NVM device was improved.<sup>12</sup> However, the induced shallow traps in the  $\text{Hf}_x\text{Al}_y\text{O}_z$  tunneling layer still affect the retention characteristics. In this paper, less shallow traps in the proposed  $\text{Hf}_x\text{Al}_y\text{O}_z$  tunneling layer could be achieved by a simple timing technique. The NVM device with proposed  $\text{Hf}_x\text{Al}_y\text{O}_z$  film will show better memory characteristics as compared to previous tunneling layer.

### Experimental

$\text{Hf}_x\text{Al}_y\text{O}_z$  films with different Al/Hf ratios (0, 0.12 and 0.278) were deposited on p-type Si substrate at 500°C by using combinations of  $\text{Hf}[\text{OC}(\text{CH}_3)_3]_2[\text{C}_5\text{H}_{11}\text{O}_2]_2$  and  $\text{Al}[\text{PCH}(\text{CH}_3)_2]_3$  precursors in metal organic chemical vapor deposition (MOCVD) system. Two precursors were injected into a pre-chamber, and then the precursors were vaporized and supplied into the main chamber by O<sub>2</sub> gas at 1500 sccm. Al/Hf ratio in  $\text{Hf}_x\text{Al}_y\text{O}_z$  film was related to respective injected times into pre-chamber. The main chamber pressure was set at 5 mbar. As shown in Fig. 1a, an interfacial layer was obtained at  $\text{Hf}_x\text{Al}_y\text{O}_z/\text{Si}$  interface. These deposited samples were called HfO<sub>2</sub>, HfAlO-1 and HfAlO-2, respectively. After  $\text{Hf}_x\text{Al}_y\text{O}_z$  deposition, a thin Pd layer was set at 2 nm and deposited by using an E-gun system ( $3 \times 10^6$  Torr, 40 mA and 0.02~0.03 nm/sec). After Pd deposition, all samples were annealed with rapid thermal annealing at 500°C for 30 sec. Then, these samples were followed by a 30-nm-thick SiO<sub>2</sub> blocking oxide deposition in plasma enhanced CVD system. The gases, power, pres-

sure and temperature were SiH<sub>4</sub>/N<sub>2</sub>O/N<sub>2</sub> (8.5/710/161.5 sccm), 20 W, 1 Torr and 300°C, respectively. The photolithography process was conducted and Al (200 nm) was deposited as the top electrodes by a lift-off technology. There was a N<sub>2</sub> annealing at 400°C after the deposition of the Al gate. In addition, some Al/Pd NCs/ $\text{Hf}_x\text{Al}_y\text{O}_z/\text{IL}/\text{Si}$  structures without blocking oxide deposition were also manufactured to compare programming current densities with one another. The energy band diagram of Al/SiO<sub>2</sub>/Pd NCs/ $\text{Hf}_x\text{Al}_y\text{O}_z/\text{IL}/\text{Si}$  structure during program operation is shown in Fig. 1b. In Results and discussion section, this energy band diagram will be used to explain the tunneling behavior.<sup>13</sup>

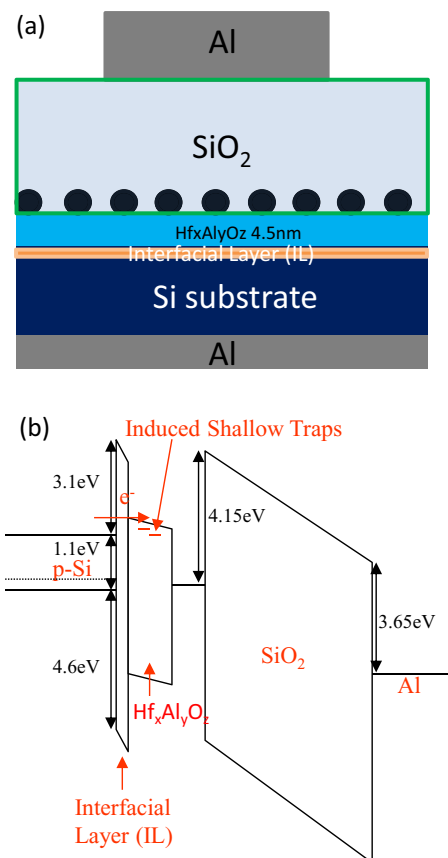


**Figure 1.** (a) Cross-sectional schematic of Al/SiO<sub>2</sub>/Pd NCs/ $\text{Hf}_x\text{Al}_y\text{O}_z/\text{IL}/\text{Si}$  (b) Energy band diagram of the structure with an interfacial layer during program operation.

\*Electrochemical Society Active Member.

<sup>z</sup>E-mail: kangtk@fcu.edu.tw

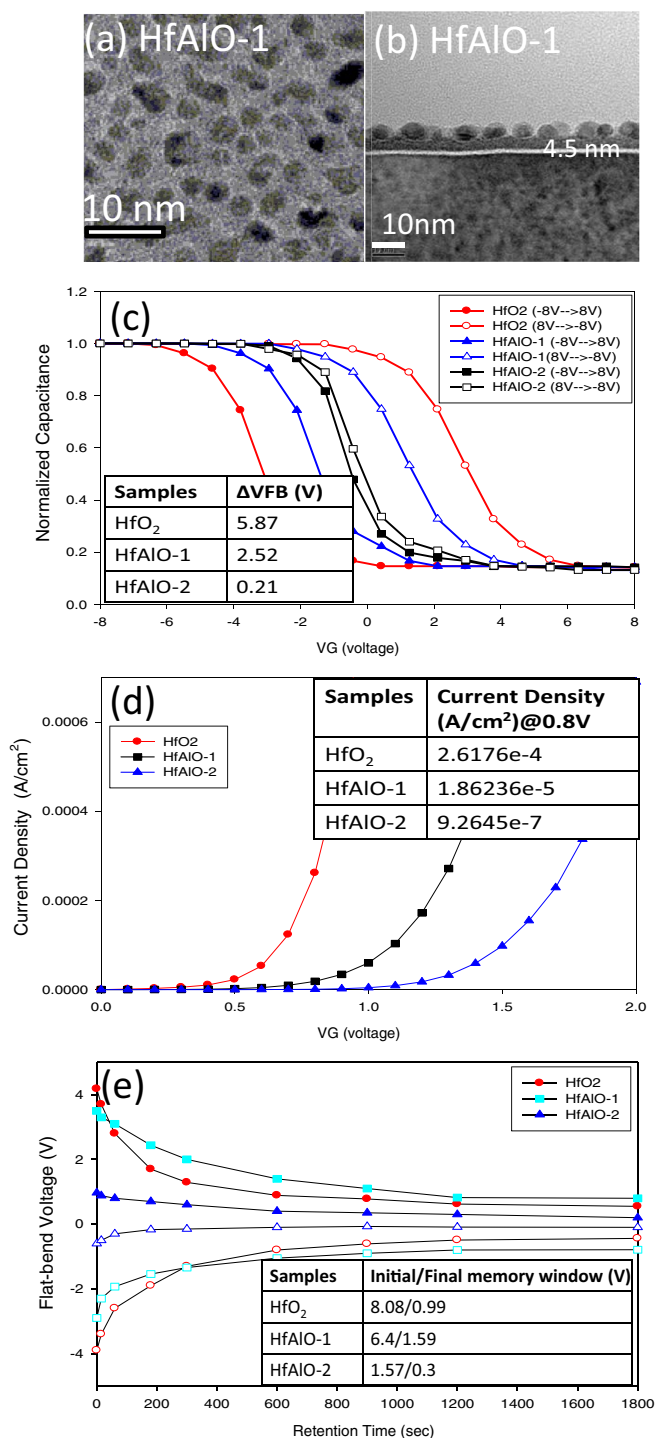


**Figure 2.** (a) TEM photograph of Pd nanocrystals on the HfAlO-1 film. (b) Cross-sectional TEM image of NVM with HfAlO-1 film. (c) Typical C-V curves with the voltage swept from 8 to -8 V and then back to 8V concerning all Al/Pd NCs/Hf<sub>x</sub>Al<sub>y</sub>O<sub>z</sub>/IL/Si structures. (d) Current densities under gate bias concerning all Al/Pd NCs/Hf<sub>x</sub>Al<sub>y</sub>O<sub>z</sub>/IL/Si structures. (e) Retention characteristics concerning all Al/SiO<sub>2</sub>/Pd NCs/Hf<sub>x</sub>Al<sub>y</sub>O<sub>z</sub>/IL/Si structures.

The capacitance-voltage (C-V) measurements were performed by a precision LCR meter of HP 4284A. In addition to LCR meter, the current measurement needs an HP 4155C parameter. The charge retention measurement adopts the C-t method.<sup>14</sup> Pd nanocrystals on different Hf<sub>x</sub>Al<sub>y</sub>O<sub>z</sub> films were inspected by transmission electron microscope (TEM) analysis. The chemical compositional analyses were conducted by Auger electron spectroscopy (AES). Regarding

the HfAlO-1 film mentioned above, two precursors have the same supply time (15 sec) and initial supply time. However, for the proposed Hf<sub>x</sub>Al<sub>y</sub>O<sub>z</sub> film, Hf[OC(CH<sub>3</sub>)<sub>3</sub>]<sub>2</sub>[C<sub>5</sub>H<sub>11</sub>O<sub>2</sub>]<sub>2</sub> precursor was first supplied and there was a 2 sec delay for the supplied Al[PCH(CH<sub>3</sub>)<sub>2</sub>]<sub>3</sub> precursor. Finally, the NVM device with the proposed Hf<sub>x</sub>Al<sub>y</sub>O<sub>z</sub> film will be fabricated and characterized.

## Results and Discussion

Pd NCs can be observed on each Hf<sub>x</sub>Al<sub>y</sub>O<sub>z</sub> film and the Pd NCs on HfAlO-1 film are shown in Fig. 2a. The density of Pd NC on each Hf<sub>x</sub>Al<sub>y</sub>O<sub>z</sub> film is about  $1.8\text{--}2.0 \times 10^{12}/\text{cm}^2$ . The cross-sectional TEM image of SiO<sub>2</sub>/HfAlO-1/IL/Si is shown in Fig. 2b. The current density of Al/SiO<sub>2</sub>/Pd NCs/Hf<sub>x</sub>Al<sub>y</sub>O<sub>z</sub>/IL/Si structure is much lower than that of Al/Pd NCs/Hf<sub>x</sub>Al<sub>y</sub>O<sub>z</sub>/IL/Si by at least 5–6 orders of magnitude. Therefore, it is considered that the charging or discharging mainly occurs between Pd nanocrystals and the Si substrate through the Hf<sub>x</sub>Al<sub>y</sub>O<sub>z</sub> tunneling layer concerning NVM device. Regarding all Al/SiO<sub>2</sub>/Pd NCs/Hf<sub>x</sub>Al<sub>y</sub>O<sub>z</sub>/IL/Si structures, the typical C-V curves with the voltage swept from 8 to -8 V and then back to 8V are obtained, as shown in Fig. 2c. A larger hysteresis is observed in these C-V curves concerning Al/SiO<sub>2</sub>/Pd NCs/HfO<sub>2</sub>/IL/Si structure, but the smallest one concerning the sample with HfAlO-2. The shallow traps in the tunneling layer can be induced from Pd NCs and they play an important role in C-V hysteresis characteristic of the NVM device.<sup>12–13</sup> According to the energy band diagram in Fig. 1b, when the voltage sweeps from 8 to -8 V, the electron is easily captured in the shal-

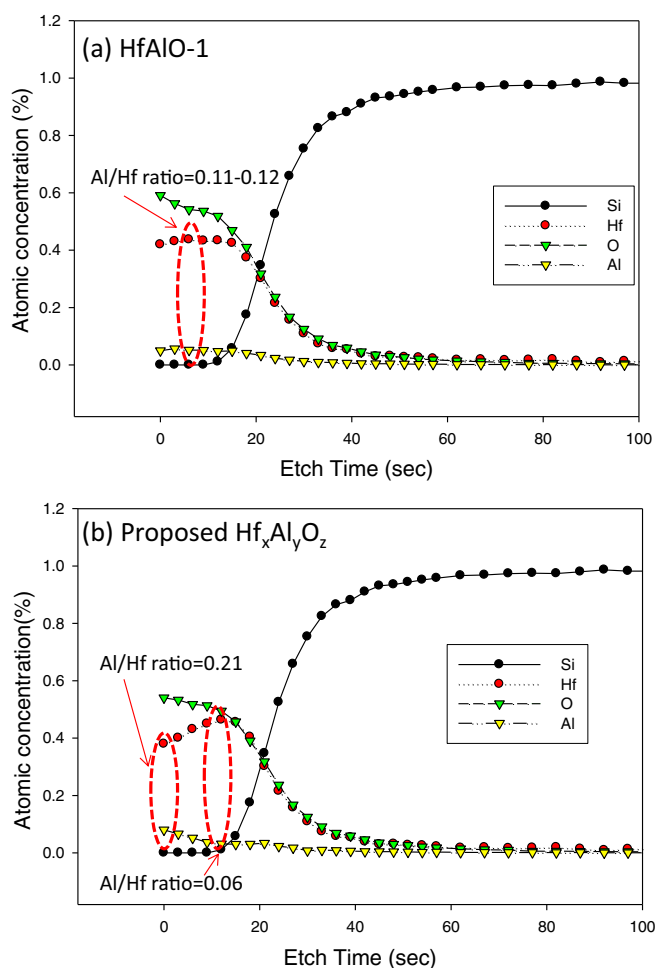


**Figure 3.** Chemical compositional analysis of the Hf<sub>x</sub>Al<sub>y</sub>O<sub>z</sub> film under the same supply time and (a) without time delay (b) with a 2 sec delay concerning Al[PCH(CH<sub>3</sub>)<sub>2</sub>]<sub>3</sub> precursor.

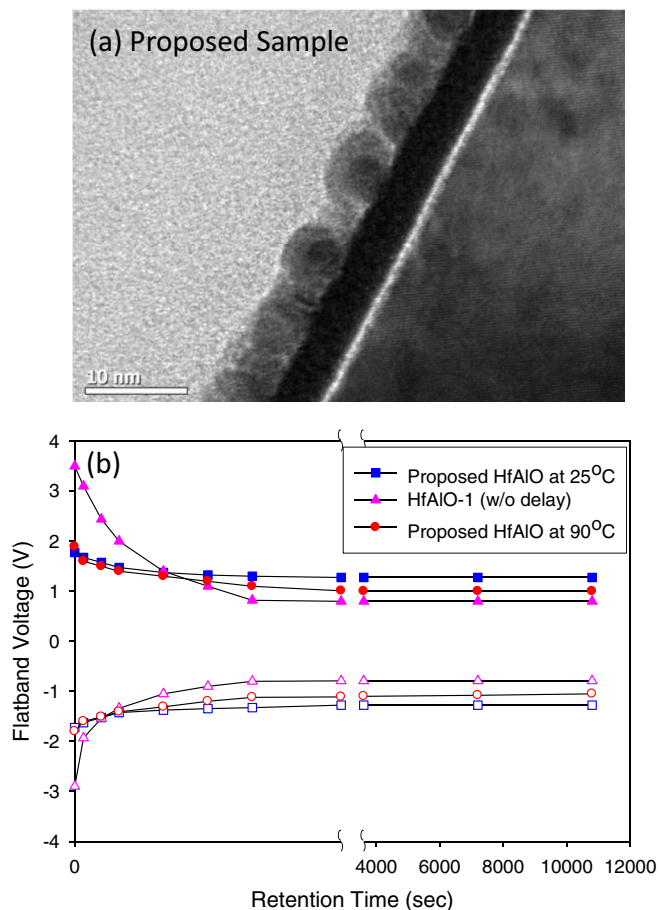


**Figure 4.** (a) Cross-sectional TEM image of NVM with proposed  $\text{Hf}_x\text{Al}_y\text{O}_z$  film. (b) Retention characteristics of the structures with/without delay concerning  $\text{Al}[\text{PCH}(\text{CH}_3)_2]_3$  precursor.

low traps of the tunneling layer and shows a positive shift in C-V curve. When the voltage sweeps from  $-8$  to  $8$  V, it is easily relaxed from the shallow traps and shows a negative shift in C-V curve.<sup>15</sup> It is considered that more induced shallow traps in  $\text{Hf}_x\text{Al}_y\text{O}_z$  film leads to a more obvious C-V hysteresis. Regarding C-V hysteresis ( $\Delta V_{\text{FB}}$ ), the summarized table is shown in the inset of Fig. 2c. Therefore,  $\text{Hf}_x\text{Al}_y\text{O}_z$  film with higher Al/Hf ratio has a better immunity to the stress from Pd NCs and a smaller C-V hysteresis is observed. For Al/Pd NCs/ $\text{Hf}_x\text{Al}_y\text{O}_z$ /IL/Si, the summarized table of the current density at  $0.8$  V is shown in the inset of Fig. 2d. It reveals that the programming current density is lower concerning the  $\text{Hf}_x\text{Al}_y\text{O}_z$  film with a higher Al/Hf ratio. Due to introducing Al to the  $\text{HfO}_2$ , it passivates the occupied  $V_{\text{O}}$  gap states and reduces leakage current paths in the  $\text{Hf}_x\text{Al}_y\text{O}_z$  film.<sup>5</sup> According to the discussion mentioned above, the NVM device with more shallow traps in  $\text{HfO}_2$  film shows a rapid drop at initial stage in retention characteristic and the least shallow traps in HfAlO-2 leads to a smallest variation of flatband voltage, as shown in Fig. 2e. Regarding initial/final memory windows, the summarized table is shown in the inset of Fig. 2e. Therefore, the  $\text{Hf}_x\text{Al}_y\text{O}_z$  film with a higher Al/Hf ratio can reduce shallow traps induced by Pd NCs to improve the retention characteristic and a lower Al/Hf ratio in the

$\text{Hf}_x\text{Al}_y\text{O}_z$  film can increase the programming current density. Regarding HfAlO-1 film, it is fabricated under the same supply time (15 sec) and initial time of Hf and Al precursors. Based on these results and discussion, the original process for HfAlO-1 film with Al/Hf ratio of 0.11–0.12 (in Fig. 3a) should be modulated. Regarding the proposed  $\text{Hf}_x\text{Al}_y\text{O}_z$  film, Hf precursor is supplied first, and then Al precursor is supplied with a 2 sec delay. As expected, Al/Hf ratio on the  $\text{Hf}_x\text{Al}_y\text{O}_z$  surface is 0.21, but only 0.06 near  $\text{Hf}_x\text{Al}_y\text{O}_z$ /IL/Si interfaces, as shown in Fig. 3b. Regarding the proposed NVM device, TEM image is shown in Fig. 4a. Owing to less induced traps in proposed  $\text{Hf}_x\text{Al}_y\text{O}_z$  film, it shows a small drop at initial stage in the retention characteristic and a final memory window of 2.5 V at  $25^\circ\text{C}$ . Moreover, a final memory window of 2.05 V at  $90^\circ\text{C}$  is also observed, as shown in Fig. 4b. Among 30 measured samples, the proposed NVM samples show that the memory windows vary from 2.3 to 2.6 V. In addition, the reliability of Al/SiO<sub>2</sub>/Pd NCs/proposed  $\text{Hf}_x\text{Al}_y\text{O}_z$ /IL/Si structure is also measured. The data endurance of the proposed memory device retains an obvious memory window of 2.4 V after  $10^4$  cycles and write/erase voltage is  $\pm 10$  V for 100 ms.

## Conclusions

Different Al/Hf ratios from 0.21 (top) to 0.06 (bottom) in the proposed  $\text{Hf}_x\text{Al}_y\text{O}_z$  tunneling layer can be fabricated. When used in NVM device, this film has less shallow traps induced by Pd NCs and provides a higher tunneling current. Regarding the proposed NVM device, the final memory windows of 2.5/2.05 V at  $25/90^\circ\text{C}$  can be achieved, respectively. When programmed and erased with  $\pm 10$  V/100 ms, the proposed NVM device shows a memory window of 2.4 V after  $10^4$  cycles for a  $25^\circ\text{C}$  test.

## Acknowledgments

The authors acknowledge National Nano Device Laboratories (NDL) for their valuable technical support. This work is also supported by the Ministry of Science and Technology under contract No. MOST-103-2221-E-035-082.

## References

- G. D. Wilk, R. M. Wallace, and J. M. Anthony, *J. Appl. Phys.*, **89**, 5243 (2001).
- R. M. Wallace and G. D. Wilk, *Crit. Rev. Solid State Mater. Sci.*, **28**, 231 (2003).
- J. Robertson, *Eur. Phys. J.: Appl. Phys.*, **28**, 265 (2004).
- W. J. Zhu, T. Tamagawa, M. Gibson, T. Furukawa, and T. P. Ma, *IEEE Electron Device Lett.*, **23**, 649 (2002).
- Quan Li, K. M. Koo, W. M. Lau, P. F. Lee, J. Y. Dai, Z. F. Hou, and X. G. Gong, *Appl. Phys. Lett.*, **88**, 182903 (2006).
- Y. N. Tan, W. K. Chim, W. K. Choi, M. S. Joo, and B. J. Cho, *IEEE Trans. Electron Devices*, **53**, 654 (2006).
- M. Takata, S. Kondoh, T. Sakaguchi, H. Choi, J. C. Shim, H. Kurino, and M. Koyanagi, *IEDM Tech. Dig.*, 553 (2003).
- S. K. Samanta, P. K. Singh, W. J. Yoo, G. Samudra, Y.-C. Yeo, L. K. Bera, and N. Balasubramanian, *IEDM Tech. Dig.*, 170 (2005).
- T. H. Hou, C. Lee, V. Narayanan, U. Ganguly, and E. C. Kan, *IEEE Trans. Electron Devices*, **53**, 3103 (2006).
- C. Lee, A. Gorur-Seetharam, and E. C. Kan, *IEDM Tech. Dig.*, 557 (2003).
- Z. Liu, C. Lee, V. Narayanan, G. Pei, and E. C. Kan, *IEEE Trans. Electron Devices*, **49**, 1606 (2002).
- Tsung-Kuei Kang, Ta-Chuan Liao, Han-Wen Liu, Fang-Hsing Wang, and Wen-Fa Wu, *Microelectronic Engineering*, **95**, 59 (2012).
- Tsung-Kuei Kang, Han-Wen Liu, Fang-Hsing Wang, Cheng-Li Lin, Ta-Chuan Liao, and Wen-Fa Wu, *Solid-State Electronics*, **61**, 100 (2011).
- C. H. Cho, B. H. Kim, T. W. Kim, S. J. Park, N. M. Park, and G. Y. Sung, *Appl. Phys. Lett.*, **86**, 143107 (2005).
- M. Houssa, M. Tuominen, M. Naili, V. Afanas'ev, A. Stesmans, S. Haukka, and M. M. Heyns, *J. Appl. Phys.*, **87**, 8615 (2000).